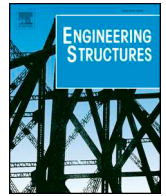




ELSEVIER

Contents lists available at ScienceDirect

Engineering Structures

journal homepage: www.elsevier.com/locate/engstruct

Experimental and numerical studies on axially loaded reinforced square hollow section T-joints

E. Ozyurt^{a,b}, S. Das^{a,*}^a Department of Civil and Environmental Engineering, University of Windsor, ON, Canada^b Department of Civil Engineering, Gumushane University, Gumushane, Turkey

ARTICLE INFO

Keywords:

Collar plate
 Doubler plate
 Full-scale tests
 Finite element analyses
 Square hollow section
 T-joints
 Ultimate capacity

ABSTRACT

This paper presents outcomes of experimental and numerical studies completed on unreinforced, collar plate reinforced and doubler plate reinforced Square Hollow Section (SHS) T-joints subjected to axial compressive loading on the brace member. A total of nine full-scale SHS T-joint specimens were fabricated and tested, in which six specimens were reinforced with collar plate and doubler plate. Non-linear finite element (FE) models were developed using finite element code, ABAQUS. Test data was used to validate these FE models. Subsequently, validated FE models were used to conduct an extensive parametric study to investigate the effect of various geometrical parameters of main members and reinforcement plates on the ultimate capacity of reinforced SHS T-joints. The parametric study found that use of both collar and doubler plate reinforcements significantly increase the ultimate capacity of SHS T-joints. Thickness of the reinforcing plate has a positive effect if the thickness of the reinforcing plate is limited to twice the thickness of the chord member. This study, however, found that the capacity of a reinforced SHS T-joint is not dependent on the type of reinforcing plate. The study concludes that the maximum capacity that can be achieved from a reinforced joint is about double the capacity of a similar unreinforced joint. It was found that the Eurocode EN 1993-1-8 overestimates the capacity of reinforced SHS T-joints. Therefore, a new design method for predicting the ultimate capacity of the collar plate and doubler plate reinforced SHS T-joints was developed and this new design method is presented in this paper.

1. Introduction

Square Hollow Section (SHS) is a popular structural element due to its excellent appearance, high strengths, and lightweight. The other advantage is that the SHS members are easy to assemble. These members have been widely used in bridges, airports, exhibition halls, roofs, and other structures. SHS members are usually connected through welding. It is worth noting that joint behaviour is more complex than member behaviour. This is because of the presence of stress concentration in and around the intersection of two SHS members [1]. Plastification of chord face commonly governs the capacity of these joints which are the most critical part of the structural components. Their ultimate capacity of SHS joints can be improved by using internal and external stiffeners. For internal stiffeners, the most common three reinforcements are grouted chord member, internal ring plate and local chord thickness reinforcements. External stiffeners are divided into two typical groups: collar plate and doubler plate. In recent years, there has been an interest in fiber reinforced polymer (FRP) reinforced tubular joints.

Several researchers have considered the effect of different geometrical parameters and different reinforcement types on the ultimate capacity of reinforced Circular Hollow Section (CHS) T-joints [2–7]. To date, there is a relatively small body of literature available on the behaviour of reinforced SHS T-joints. Feng et al. [8] examined the effect of the collar and doubler plate reinforcement on the strength of SHS T-joint and the study used both experimental and numerical techniques. The study, based on the numerical results, proposed a correction factor for the current design method of unreinforced SHS T-joints for predicting the capacity of reinforced SHS T-joints. However, the correction factor for the doubler plate reinforced SHS T-joints was given a negative value on the reinforced joints compared to the unreinforced ones when the brace-to-chord width ratio is between 0.3 and 0.85.

Currently, there are no design recommendations available specifically for predicting the ultimate capacity of reinforced tubular joints. However, Eurocode 3 EN 1993-1-8 [9] suggests that for chord face failure, brace failure, and punching shear failure, the capacity of reinforced SHS T-joints can be determined using the design equation

* Corresponding author.

E-mail address: sdas@uwindsor.ca (S. Das).<https://doi.org/10.1016/j.engstruct.2019.05.012>

Received 4 December 2018; Received in revised form 1 April 2019; Accepted 5 May 2019

0141-0296/ © 2019 Elsevier Ltd. All rights reserved.

Notations			
<i>The following symbols are used in this paper:</i>		n	chord stress parameter
L_0	length of chord	t_0	wall thickness of chord
L_1	length of brace	t_1	wall thickness of brace
L_r	length of reinforcement	t_r	thickness of reinforcement
N_u	unreinforced joint capacity of axially loaded SHS T-joints	β	diameter ratio ($= b_1/b_0$)
N_r	reinforced joint capacity of axially loaded SHS T-joints	θ	brace-to-chord intersection angle
Q_f	function to take account of the effect of chord stress in the connecting face	γ	half width to thickness ratio of the chord ($= b_0/2t_0$)
Q_u	function in the design strength equations accounting for the effect of geometric parameters	η	brace depth h_1 (in direction chord axis) to chord width (b_0) ratio
b_0	external width of chord member	λ	doubler or collar plate length (L_r) to chord width (b_0) ratio
b_1	external width of brace member	Δ	doubler or collar plate thickness (t_r) to chord member thickness (t_0) ratio
$f_{y,0}$	yield stress of chord member	ε	engineering strain
h_0	external depth of chord member	ε_i	strain
h_1	external depth of brace member	ε_T	true strain
		σ	engineering stress
		σ_T	true stress

recommended for the unreinforced SHS T-joints and replacing the chord wall thickness with the reinforced plate thickness. Thus, according to this method, the capacity of reinforced joints compared to the unreinforced joints will be increased by the square of the thickness of the reinforced plate as shown in Eq. (3). Hence, the capacity of the T-joint reinforced with doubler plate will be predicted to be increased by four times as compared to the unreinforced T-joint when the doubler plate thickness is twice the chord member thickness. This prediction is in contrary to previous studies [2,10] which have reported that the capacity of doubler or collar plate reinforced tubular CHS T-joints under brace axial compressive load can be increased up to two-fold compared to their unreinforced capacity. Therefore, the current design guideline of EN 1993-1-8 may be un-conservative and unsafe for reinforced SHS T-joints.

Previous studies mainly focused on externally reinforced CHS joints, because it is easier to reinforce joints using external stiffeners rather than using internal stiffeners [11–15]. The literature review found that there is a lack of study on SHS T-joints reinforced with doubler plate and collar plate. Therefore, this study was designed and executed to determine the structural behaviour and ultimate load capacity of SHS T-joints reinforced with doubler plate and collar plate. Identical unreinforced SHS T-joints were also tested for comparisons. Firstly, the experimental work was carried out to investigate the effects of different reinforcement methods: doubler plate and collar plate on the capacity of SHS T-joint. Next, a parametric study using validated finite element (FE) models was carried out to examine the effect of various geometrical parameters for main members and reinforced plates on the ultimate load capacity of SHS T-joint. Using the results of the parametric study a new design equation for predicting the capacity of these joints was developed and it is presented in this paper.

Table 1
Geometrical dimensions of test specimens (all dimensions in mm).

Specimen	Chord member				Brace member				Reinforced plate			$\beta (= b_1/b_0)$
	b_0	h_0	t_0	L_0	b_1	h_1	t_1	L_1	L_r	b_r	t_r	
U1	102	102	4.8	1001	51	51	4.8	500	–	–	–	0.50
C1-6	102	102	4.8	1001	51	51	4.8	500	151	101	6	0.50
D1-6	102	102	4.8	1002	51	51	4.8	500	151	101	6	0.50
U2	102	102	4.8	1200	76	76	4.8	500	–	–	–	0.75
D2-6	102	102	4.8	1200	76	76	4.8	500	151	101	6	0.75
D2-12	102	102	4.8	1200	76	76	4.8	500	149	101	12	0.75
U3	76	76	4.8	1200	51	51	4.8	450	–	–	–	0.67
D3-6	76	76	4.8	1200	51	51	4.8	450	148	75	6	0.67
D3-12	76	76	4.8	1200	51	51	4.8	450	148	75	12	0.67

2. Experimental work

2.1. Specimens and test setup

Table 1 shows the test matrix used in this study. As can be found from this table, nine full-scale SHS T-joint specimens were fabricated and tested. These specimens included three unreinforced joints (specimens U1, U2, and U3), one collar plate reinforced joint specimen (specimen C1-6) and five doubler plate reinforced joint specimens (specimens D1-6, D2-6, D2-12, D3-6, and D3-12). The unreinforced joint specimens are used as reference specimens for determining the comparative behaviour and capacities of the reinforced SHS T-joints. As can be found that the thickness of the reinforced plates and the type of the reinforcement plates were varied in the experimental study.

Since the wall thickness of the brace member has an insignificant effect on the ultimate capacity of tubular joints [16], the brace wall thickness was not varied in the test specimens. However, brace-to-chord width ratio (β) has a significant impact on the tubular joint strength. Therefore, three different brace-to-chord width ratios ($\beta = 0.50, 0.67$ and 0.75) were considered in the test matrix (Table 1). The geometrical dimensions chosen in this study are within the range of recommended values of the CIDECT guide No. 3 [17] and EN 1993-1-8 [9]. In order to exclude the effect of the boundary condition on the structural behaviour of tubular joints, Shao et al. [18] recommended that a chord length (L_0) needs to be about 10 times or larger than the chord member width, b_0 . Hence, the chord lengths chosen in this study were about or larger than $10b_0$. The wall thickness of the chord and brace members was kept unchanged at 4.8 mm.

According to the Eurocode 3 EN 1993-1-8 [9], the minimum length and width of the reinforcement plate can be determined from Eqs. (1)

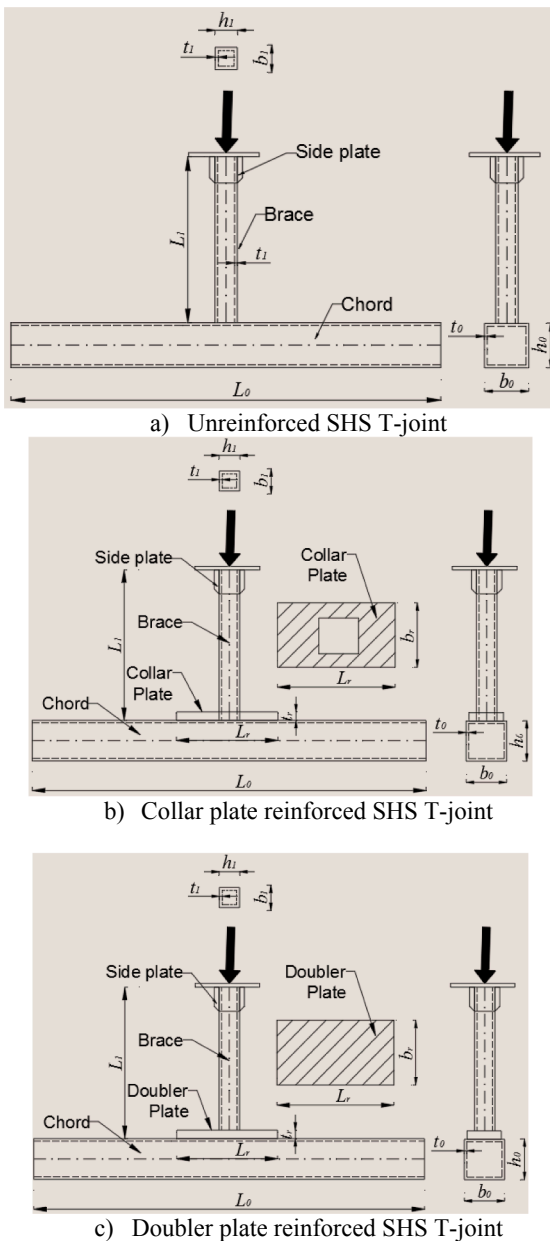


Fig. 1. Configurations of unreinforced and reinforced SHS T-joints.

and (2), respectively. The geometrical parameters of both collar and doubler plates were selected based on the recommendation of the Eurocode 3 EN 1993-1-8 [9]. The capacity of unreinforced welded tubular T-joints (N_u) when β is less than or equal to 0.85 can be calculated by using Eq. (3) available in the Eurocode EN 1993-1-8 [9]. Fig. 1 illustrates the typical unreinforced and reinforced joint configurations.

$$L_r \geq h_1 + \sqrt{b_r(b_r - b_1)} \quad (1)$$

$$b_r \geq b_0 - 2t_0 \quad (2)$$

$$N_u = \frac{f_{y,0} t_0^2}{1 - \beta} (2\beta + 4\sqrt{1 - \beta}) \quad (3)$$

where $f_{y,0}$ is the yield strength of chord member and β is the diameter ratio ($= b_1/b_0$).

The mechanical properties of steel material used in the tests are tabulated from the tests of coupon specimens in Table 2.

Fig. 2 shows the experimental setup of a typical specimen. The clear

distance between the bottom supports was 840 mm, while the centre-to-centre distance between the pin and roller was 1000 mm. One end plate for each specimen was welded at the top end of brace member to facilitate the application of axial load. The axial load was applied by a hydraulic actuator with a maximum load capacity of 250 kN. In order to avoid any local buckling at the end of the brace member, the short side plates were welded on all the four faces of the brace member as illustrated in Fig. 1. Chord member was supported by a roller at one end and a pin at the other end as shown in Fig. 2b and c, respectively.

Fig. 3 shows the locations of the linear variable differential transformers (LVDT) and strain gauges. LVDT D1 measured the local deformation at the top surface of the chord member; LVDT D2 measured horizontal (lateral) displacement of the side wall of the chord member at its mid-span; LVDT D3, LVDT D4, and LVDT D5 measured the vertical displacement of the chord member's bottom surface at each 1/4th span as illustrated in Fig. 3a. Ten strain gauges were installed at and around the intersection of chord and brace members. Strain gauges T1 and T2 were installed on the surface of the brace member facing vertical direction; strain gauges T3–T6 were placed at the top surface of the chord member for unreinforced joints, while for reinforced specimens, strain gauge T3 was installed on the reinforcement plate; strain gauges T7–T10 were placed on the side wall of the chord member as shown in Fig. 3b. The distance between the weld toe and strain gauge T3 for each specimen was 20 mm.

2.2. Test results

This section presents the test data, including the load-ovalization displacement curves, failure modes and ultimate capacity of unreinforced and reinforced SHS T-joints.

Fig. 4 illustrates the failure mode of each specimen. All test specimens failed due to local plastic deformation of the chord face. For the unreinforced joints, the plastic deformation occurred around the brace-to-chord intersection area (Fig. 4a, d, and g), while plastic deformation took place at the toe of the reinforcement plate of the specimens reinforced with both collar plate and doubler plate (Fig. 4b, c, e, f, h and i). When the unreinforced tubular joints were under the axial compressive load, large deformations took place at the top surface of the chord in the intersection area, resulting in an outward deformation (local bulging) of the side wall of the chord member. For specimens reinforced with collar plate and doubler plate, the location of the plastic deformation moved from brace-to-chord intersection area away to the toe of the reinforcement plate. Hence, the location of plastic deformation moved and the capacity of the reinforced joints increased significantly as shown in Fig. 5.

Fig. 5 presents the load-ovalization displacement curves of the unreinforced joint (U1), joint reinforced with a collar plate (C1-6) and joint reinforced with a doubler plate (D1-6). The ovalization displacement was measured as the difference in displacements measured at the bottom surface of the chord member (LVDT D3, see Fig. 3a) and the top

Table 2

Mechanical properties of steel materials used in the test.

Specimen (mm)	Coupon ID	f_y (MPa)	f_u (MPa)	E (GPa)
102 × 102 × 4.8	A1	277	420	265.0
	A2	286	421	279.8
	Mean	281.5	420.5	272.4
76 × 76 × 4.8	B1	357	429	236.9
	B2	379	447	221.8
	Mean	368	438	229.3
51 × 512 × 4.8	C1	388	436	250.3
	C2	410	440	216.4
	Mean	399	438	233.3
Plates	P1	578	587	230.0

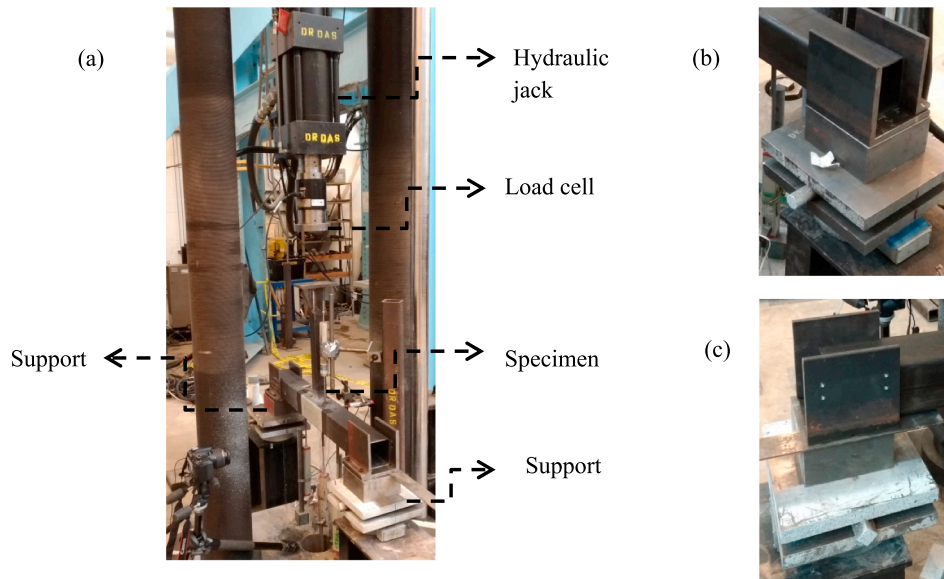


Fig. 2. Experimental setup of an axially loaded SHS T-joint; (a) Test arrangement, (b) Roller Support, (c) Pin support.

of the chord member (LVDT D1, see Fig. 3a). The typical failure mode for tubular joints is due to plastic deformation in the chord member. Premature failure of brace member and weld did not occur in any specimen. Therefore, it is important to illustrate the behaviour of tubular joints with joint displacement instead of the displacement of the vertical brace member. Fig. 5 also shows a deformation limit which was recommended by Lu et al. [19] and this limit is shown by a broken vertical line in this figure. Based on the deformation limit of Lu et al. [19], the capacity of a tubular joint is considered as the peak load if the peak load occurs before reaching 3% deformation of the chord member. However, if the peak load occurs beyond 3% deformation, the capacity of tubular joint is considered as the value of the load when the deformation of the chord member reaches 3%. If this limit exceeded

before the peak load, the applied load corresponding to $0.03h_o$ was defined as the capacity. As can be found from Fig. 5, the capacity of the reinforced SHS T-joints increased by almost 200% if compared with the capacity of the unreinforced joint. It can be also noted that the behaviours of the joints reinforced with collar plate and doubler plate were similar.

2.3. Strain distribution

Ten strain gauges were installed around the brace-to-chord intersection to understand the behaviour of reinforced SHS T-joints as illustrated in Fig. 3. Fig. 6 shows the strain distribution curves at the different load levels. There are two curves in each plot. One curve

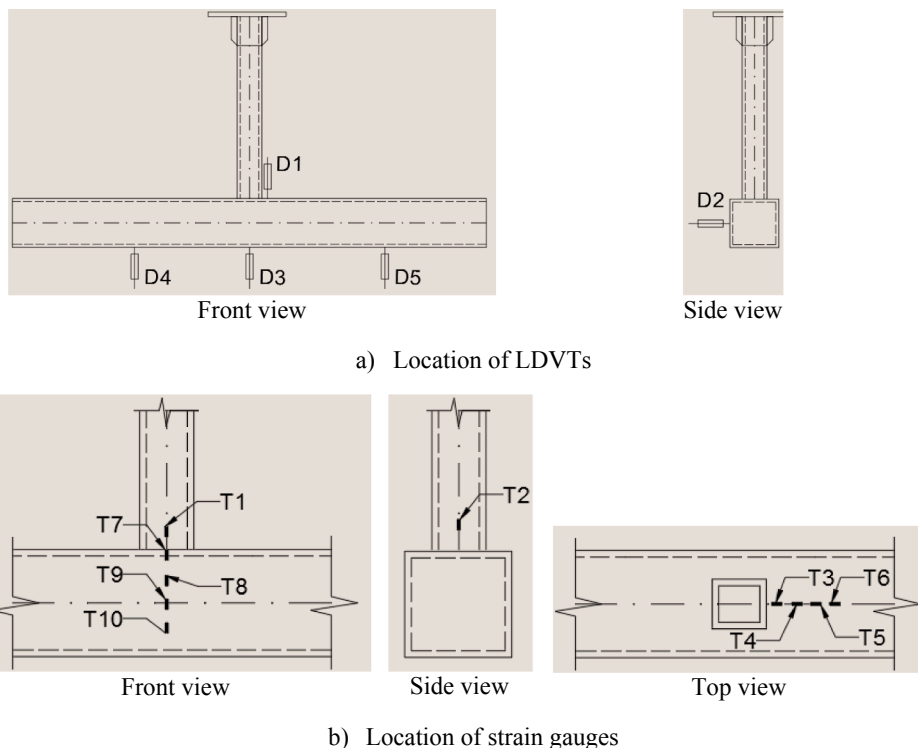


Fig. 3. Locations of LDVTs and strain gauges.

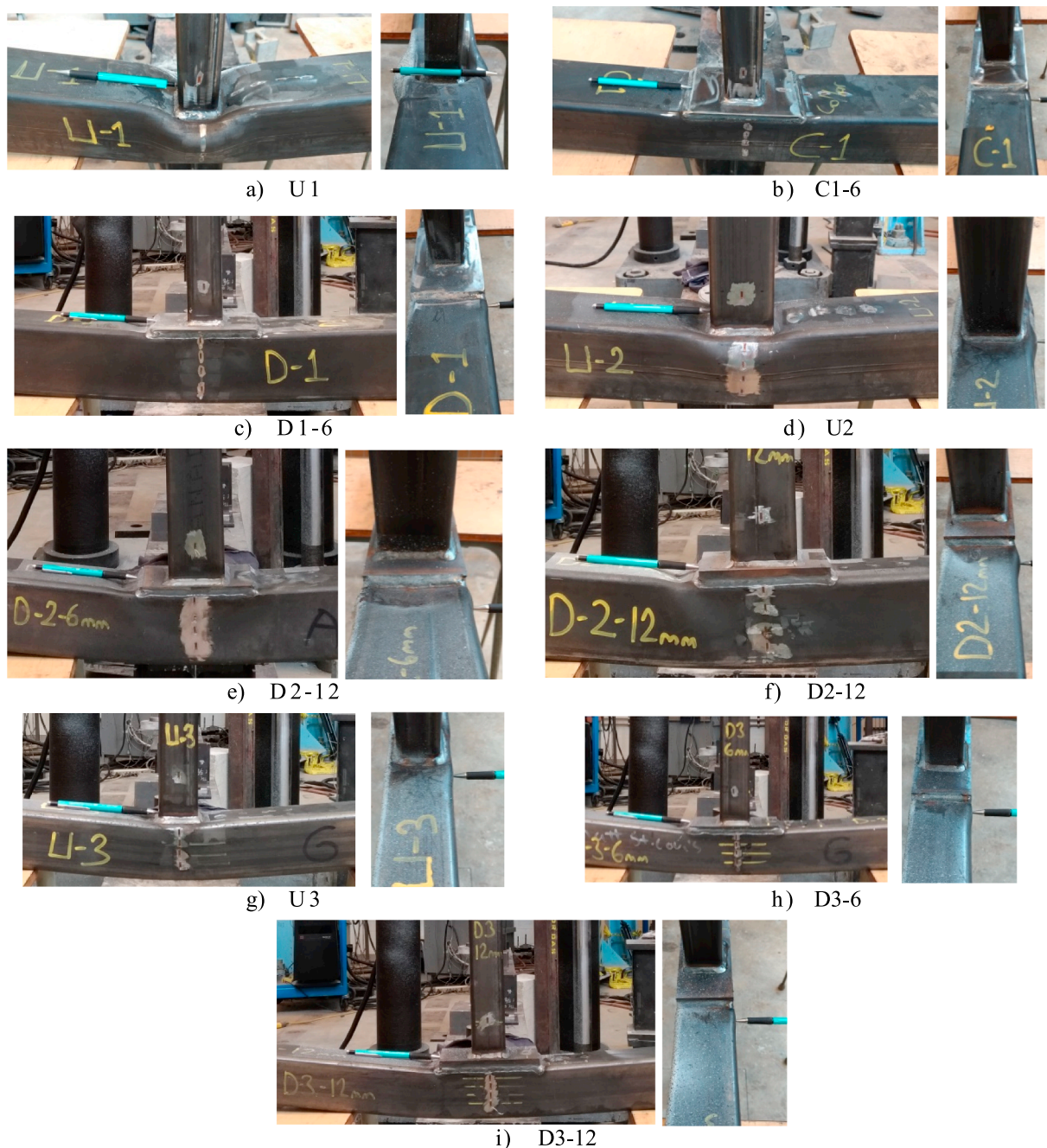


Fig. 4. Deformed shape of tested joints.

represents that strain distribution at the yield load (when the first strain gauge reached yielding strain) while the other curve indicates the strain distribution at the ultimate load which is the peak load in the load-displacement curves. The yield load is defined from the load-displacement curves as suggested by Kurobane et al. [20]. Strain gauges T6 for specimen U1, T3 for specimen D2-6, T10 for specimen U3 and T9 for specimen D3-12 failed at the preparation stage of the specimens. Fig. 6 shows that there was no yielding at the brace member (strain gauges T1 and T2 in Fig. 3b) for all unreinforced and reinforced SHS T-joints. However, it can be noted that for unreinforced joints (specimens U1, U2, and U3) the deformations at the top surface of the chord member (strain gauge T2-T6 in Fig. 3b) and side wall of the chord member (strain gauges T7-T10 in Fig. 3b) were higher at the ultimate load, while the strains for the reinforced joints were more severe at the top surface of the chord. It can be clearly observed from the strain curves of

unreinforced joints (specimens U1-U3) that the yielding first occurred at strain gauge T3 which was located at the weld toe. However, for the reinforced joints, the yielding first occurred at strain gauge T4 which was placed at the toe of the reinforcing plate toe. Fig. 6 also demonstrates that the strain values for the joints reinforced with doubler plate were slightly less than the strains of the joints reinforced with collar plate. This is due to the fact that the joints reinforced with doubler plates have a higher stiffness around the intersection area. The research has also shown that the failure of the un-reinforced joints was due to a combination of chord top surface and chord side-wall failures, while the reinforced joints failed because of chord top surface failure.

2.4. Comparison of the test results with the current design method

Currently, design codes and standards do not recommend any

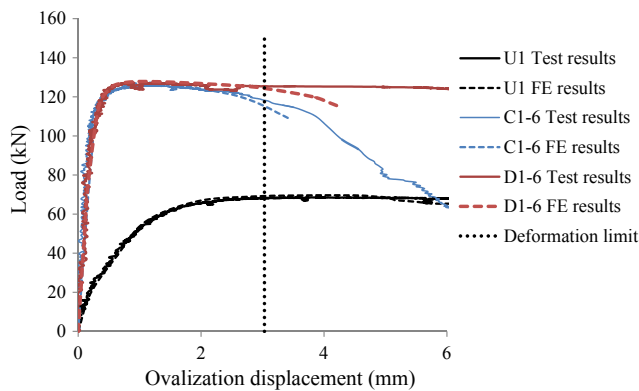


Fig. 5. Comparison of load-ovalization curves of test specimens with those of FE results.

Table 3
Comparison of the test results with the EN 1993-1-8 [9].

Specimen	Test results of N_u to N_r ratio	N_u to N_r ratio based on EN 1993-1-8 [9]
U1	–	–
C1-6 ($t_p/t_r = 1.25$)	1.83	1.56
D1-6 ($t_p/t_r = 1.25$)	1.85	1.56
U2	–	–
D2-6 ($t_p/t_r = 1.25$)	1.21	1.56
D2-12 ($t_p/t_r = 2.5$)	1.18	6.25
U3	–	–
D3-6 ($t_p/t_r = 1.25$)	1.14	1.56
D3-12 ($t_p/t_r = 2.5$)	1.17	6.25

design equations for calculating the capacity of reinforced tubular joints. However, the British Standard [9] recommends using Eq. (3) available in the Eurocode EN 1993-1-8 [9] for unreinforced tubular joints by replacing the chord thickness (t_c) with the reinforced plate thickness (t_r) for predicting the capacity of reinforced welded tubular joints when failure occurs either at the chord face, or at the brace, or due to punching shear.

Table 3 compares the test results along with the predictions of the EN 1993-1-8 [9]. According to the current method, the capacity of the reinforced welded tubular T-joints (N_r) increases by the proportion of the square of the reinforcing plate thickness to the square of the member thickness (see Eq. (3)). For example, the capacity of the reinforced joint is four times higher than the corresponding unreinforced joint when the reinforcing plate thickness is twice the thickness of the chord member.

Hence, the ratios of the unreinforced joint capacity to reinforced joint capacity were used for both the test results and predictions of the EN 1993-1-8 [9] in Table 3. This table shows that the current design guideline of EN 1993-1-8 is unable to predict the ultimate load capacity of the SHS T-joints reinforced with collar plate and doubler plate. The predictions of the EN 1993-1-8 [9] for C1-6 and D1-6 joints were conservative. However, for other joints, predictions by EN 1993-1-8 [9] were unconservative or unsafe. The most striking result emerges from specimens D2-12 and D3-12. The Eurocode, EN 1993-1-8 [9] suggests that the reinforced joint capacity should be 6.25 times to that of the capacity of the unreinforced joint. However, the test results of this study indicate that the capacities for these two reinforced specimens are only 1.17 and 1.18 times, respectively.

The objective of this study is to determine the capacity of the collar plate and doubler plate SHS T-joints and propose a safe method to calculate the capacity of reinforced tubular joints. The objective is achieved using the results of Finite Element (FE) analyses which is undertaken using commercially available FE software, ABAQUS v6.14

[21]. The FE models are validated using the test results. Validated FE models are then used to undertake an extensive parametric study considering various geometrical parameters of the member and reinforcing plates is carried out. Based on the test data and numerical results, a new design method for calculating the capacity of reinforced welded SHS T-joints is developed and presented in this paper.

2.5. Finite element modelling

The experimental results were used to validate the numerical (FE) models. Fig. 1 shows the geometric configuration of unreinforced, collar plate reinforced and doubler plate reinforced SHS T-joints. To reduce computational time, a half of T-joint along its length was modeled using the symmetry in the geometry, boundary condition, and loading. Fig. 7 shows numerical models for the unreinforced and reinforced SHS T-joints tested. Three-dimensional eight-node solid elements with incompatible modes (C3D8I) were used for the chord, brace members, reinforced plates and weld geometry. The same modelling parameters were used for the reinforced tubular joints by other researchers to save computational time [4,8,22,23]. Similar to the experiments, short plates were attached on all four surfaces of the brace member for both un-reinforced and reinforced joints as shown in Fig. 7a–c. A rigid plate was modelled at the top surface of the brace member using a tie for application of axial load on the brace member. The same tie was also used for connecting the reinforcement plates and members with the weld elements. For simulating the boundary conditions to the test specimens, the middle lines under the bottom supports at one end of the chord was restrained as a roller support and the other end of the chord was restrained as a pin support as shown in Fig. 7a–c.

The Riks method was chosen to apply the mechanical loads and examine the effects of large deformations after reaching the ultimate capacity in the joints. The axial brace loads were applied in small increments to achieve the numerical convergence in the non-linear joint behaviour.

For the verification of the numerical models, the material properties of the members and plates were based on the average value of the tensile coupon test results. In the FE models, the true stress-strain curve was input after converting the engineering stress-strain curve in the tensile coupon tests into the true stress and logarithmic strain curve using Eqs. (4) and (5) [24]. In all numerical analyses, the von-Mises yield criterion and isotropic strain hardening rules were used.

$$\varepsilon_T = \ln(1 + \varepsilon) \quad (4)$$

$$\sigma_T = \sigma(1 + \varepsilon) \quad (5)$$

where

- ε_T is the true strain
- ε is the engineering strain
- σ_T is the true stress
- σ is the engineering stress

A mesh convergence study was carried out to determine the optimum mesh size for accuracy of the results and as well as for an acceptable computational time. Mesh sizes of about twice the chord thickness and about chord wall thickness were used in the region of outside the joint zone and brace to chord intersection region of the tubular members, respectively. For reinforced plates, a finer mesh (0.1969 in or 5 mm) was used. The brace and chord members were tied with the weld elements. Discretization method was defined as a surface to surface contact. The brace and chord members at the connection region were chosen as a master surface, while the weld elements were slave surface.

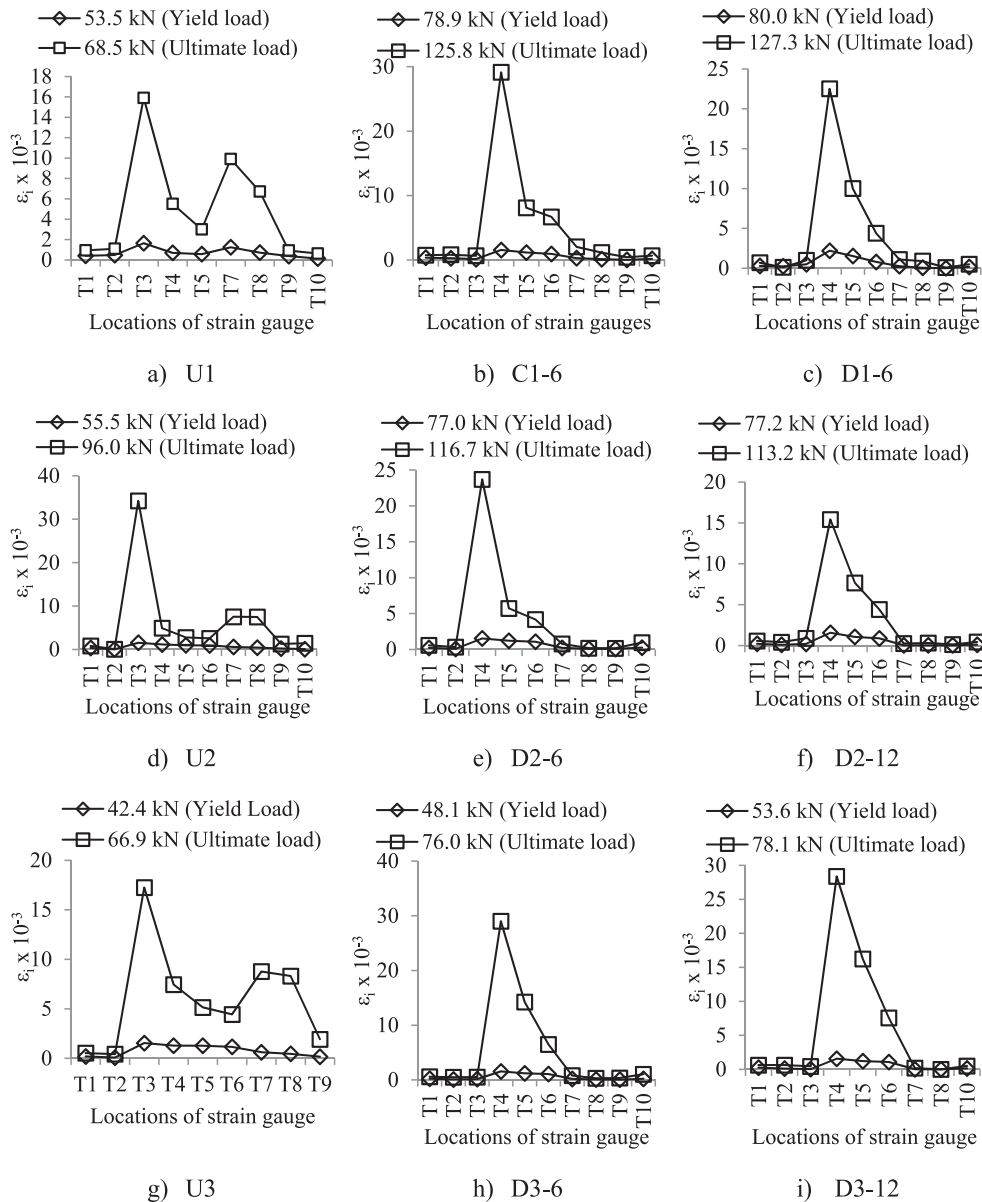


Fig. 6. Strain distributions at different load levels.

2.6. Validation of finite element models

This section presents the validation of the failure modes, load-ovalization displacement curves, strains in the elastic range and the ultimate load. Fig. 8 compares the selected failure mode shapes between the test specimens and the FE models. The deformed shapes of the joints of the FE models were similar to that of the test specimens as can be seen from Fig. 8. In both cases, the failure was due to plastification of the chord face.

Fig. 5 compares the load-ovalization displacement curves of the selected joints obtained from the tests and FE analyses. A good correlation between the tests and FE results are found. The vertical broken line in Fig. 5 is the deformation limit proposed by Lu et al. [19]. Table 4 presents the ultimate capacity of all joints as obtained from the tests and FE models. A good agreement between the test and numerical results is observed. Furthermore, Fig. 9 illustrates a comparison for strains of unreinforced (U1) and reinforced (C1-6) joints in the elastic range between the test and FE results. The strain values were picked when the applied load at the top of the brace member was 45 kN. As can be found that a good agreement between the test and FE results were achieved.

3. Parametric study and results

The validated FE models were used for a detailed parametric study to determine the effect of various geometric parameters on the ultimate load capacity of axially loaded SHS T-joints reinforced with collar and doubler plates as shown in Fig. 1. Fig. 10 presents the loading and boundary conditions used in all FE models used in this parametric study. Both geometry and material non-linearities were considered. In order to examine large deformation behaviour, the RIKS method was chosen. When the arc length increments were within the maximum and minimum limitations of 0.1 and 1E-015 respectively, numerical convergence was considered to have been achieved. In all numerical models, the steel grade was S355J2H EN 10,210 with an actual yield strength = 355 N/mm² and an ultimate strength = 510 N/mm². The elastic modulus of steel was 210 GPa. For the weld material, the same material properties as a chord and brace members were used.

There is a large volume of published studies describing the effect of geometrical parameters on the capacities of unreinforced tubular joints [25–29]. The geometrical parameters used in these studies were β ($= b_1/b_0$), γ ($= b_0/2t_0$) and τ ($= t_1/t_0$). For reinforced tubular joints, the

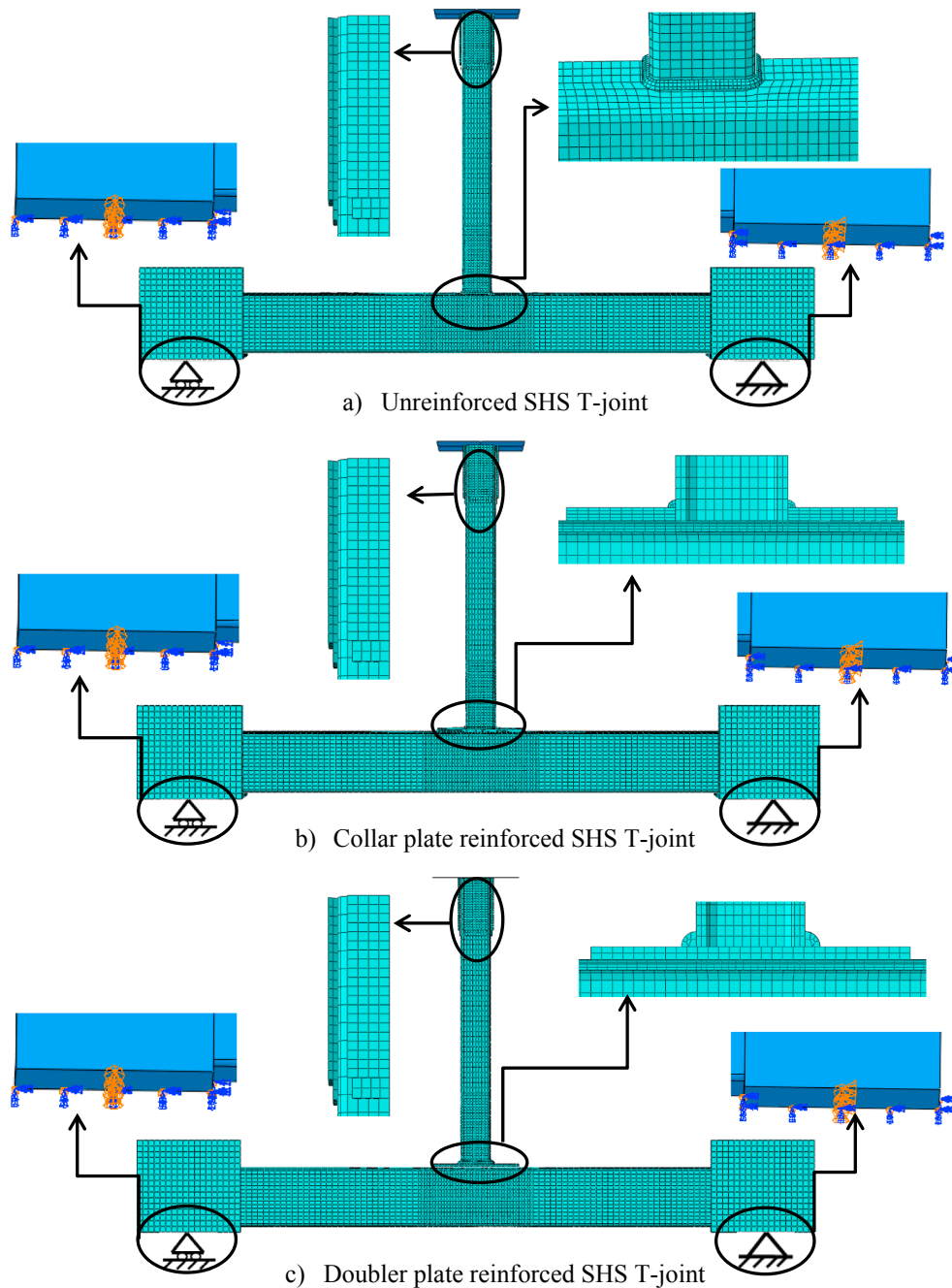


Fig. 7. Mesh layouts and boundary conditions of numerical models.

previous studies mainly examined the effect of reinforced plate length and reinforced plate thickness on the ultimate capacity [3,8,10,13,30]. Since parameters γ and τ relate to t_0 for unreinforced joints and t_r is replaced with t_r for reinforced joints, the effects of non-dimensional parameters β , Δ and λ on the ultimate capacity of reinforced SHS T-joints have been investigated. The FE models for unreinforced and reinforced joints are labeled as follows:

- Designation of the unreinforced joints is L1-N1. The first letter (L1) represents the reinforcing plate type (L1 = U for unreinforced joints). The following number (N1) indicates the simulated joint case.
- Designation of the reinforced joints is L1-N1-N2-N3. The first letter (L1) refers to the reinforcement type (C for collar plate reinforcement or D for doubler plate reinforcement). The first number (N1) is for the joint case. The subsequent number (N2) indicates the ratio of

reinforced plate length to chord member width ($N2 = \lambda = L_r/b_0$). The last number (N3) refers to the ratio of the reinforced plate thickness to chord member thickness ($N3 = \Delta = t_r/t_0$).

Table 5 summarises the geometrical parameters of all unreinforced, collar plate reinforced and doubler plate reinforced SHS T-joints considered in the parametric study. The geometrical dimensions were within the range of validity in accordance with CIDECT guide No. 3 [17] and EN 1993-1-8 [9]. According to these standards, for reinforced joints, t_0 should be replaced by t_r in the case of chord face failure, brace failure, and punching shear failure [9]. The chord length and brace length for all FE models were 2000 mm and 1000 mm, respectively.

Since the current design method of Eurocode EN 1993-1-8 [9] for calculating the capacity of reinforced SHS T-joints may not be safe, the

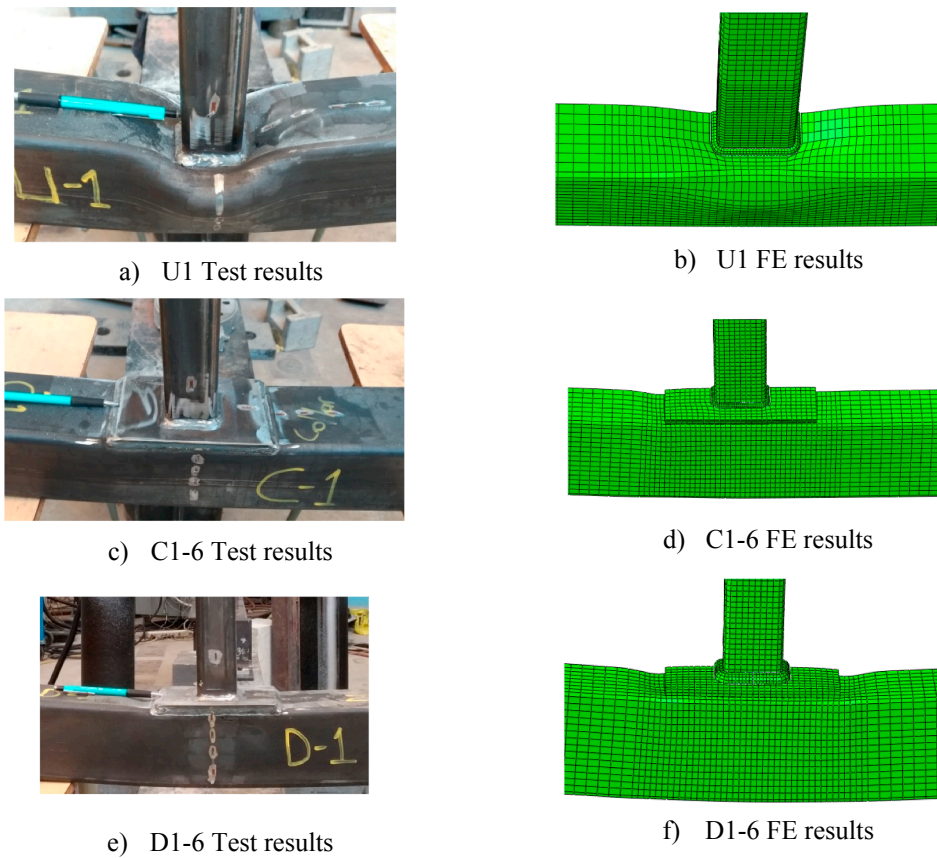


Fig. 8. Comparison of failure mode shapes of selected joints of FE results with the test results.

Table 4
Comparison of the ultimate capacities of tested joints with those of FE models.

Specimen	Test results (kN)	FE results (kN)	Ratio (FE result/Test results)
U1	68.5	69.6	1.02
C1-6	125.8	127.2	1.01
D1-6	127.3	127.9	1.00
U2	96.0	99.8	1.04
D2-6	116.7	120.2	1.03
D2-12	113.2	112.1	0.99
U3	66.9	70.1	1.05
D3-6	76.0	76.7	0.99
D3-12	78.1	80.4	1.03

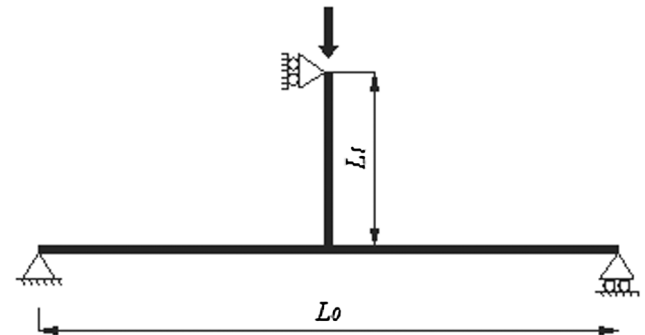


Fig. 10. Boundary conditions of numerical models.

3.1. Assessment of SHS T-joints with collar and doubler plates

A total of 76 FE models of SHS T-joints reinforced with collar and doubler plates, considering different geometrical parameters were analyzed in order to study the effects of the different reinforcing plate types on the ultimate capacity of reinforced SHS T-joints under axial brace compressive loading. The geometrical parameters for each joint are summarized in Table 5. Fig. 11 illustrates a comparison of the ultimate capacity of the collar plate SHS T-joints reinforced with collar plate with same SHS T-joints reinforced with doubler plate. The results of this study indicate that there is no significant differences between the ultimate capacity of a collar plate reinforced SHS T-joint and a doubler plate reinforced SHS T-joint. Moreover, the failure mode of both doubler plate or collar plate reinforced joints is due to the chord face plastification. This also accords with the test observations, which showed that the ultimate capacity of the reinforced joints was independent of the type of the reinforcing plates. Therefore, this study recommends using doubler plate

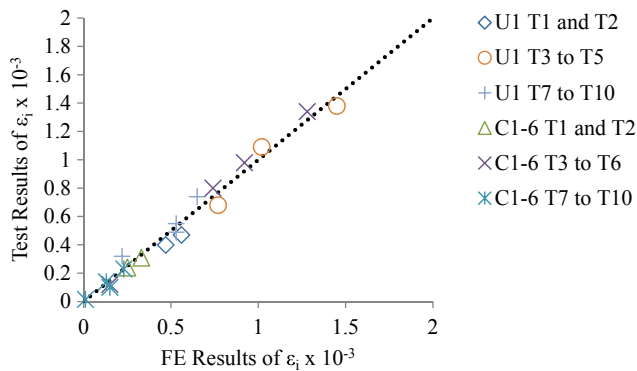


Fig. 9. Comparison of strains at different locations of specimens.

following sections discuss the effect of reinforcing plate types and various geometrical parameters of both reinforcing plates and tubular members on the capacity of reinforced welded SHS T-joints.

Table 5
Geometrical parameters of numerical models.

Specimen	Chord member		Brace member		Reinforced plate			β	Δ	λ
	b_0 and h_0	t_0	b_1 and h_1	t_1	L_r	b_r	t_r			
U-1	200	8.0	60	8.0	–	–	–	0.30	–	–
C-1-1.25-1	200	8.0	60	8.0	250	185	8	0.30	1.00	1.25
D-1-1.25-1	200	8.0	60	8.0	250	185	8	0.30	1.00	1.25
C-1-1.25-2	200	8.0	60	8.0	250	185	16	0.30	2.00	1.25
D-1-1.25-2	200	8.0	60	8.0	250	185	16	0.30	2.00	1.25
C-1-1.25-3	200	8.0	60	8.0	250	185	24	0.30	3.00	1.25
D-1-1.25-3	200	8.0	60	8.0	250	185	24	0.30	3.00	1.25
C-1-2-1	200	8.0	60	8.0	400	185	8	0.30	1.00	2.00
D-1-2-1	200	8.0	60	8.0	400	185	8	0.30	1.00	2.00
C-1-2-2	200	8.0	60	8.0	400	185	16	0.30	2.00	2.00
D-1-2-2	200	8.0	60	8.0	400	185	16	0.30	2.00	2.00
C-1-2-3	200	8.0	60	8.0	400	185	24	0.30	3.00	2.00
D-1-2-3	200	8.0	60	8.0	400	185	24	0.30	3.00	2.00
C-1-2.5-1	200	8.0	60	8.0	500	185	8	0.30	1.00	2.50
D-1-2.5-1	200	8.0	60	8.0	500	185	8	0.30	1.00	2.50
C-1-2.5-2	200	8.0	60	8.0	500	185	16	0.30	2.00	2.50
D-1-2.5-2	200	8.0	60	8.0	500	185	16	0.30	2.00	2.50
C-1-2.5-3	200	8.0	60	8.0	500	185	24	0.30	3.00	2.50
D-1-2.5-3	200	8.0	60	8.0	500	185	24	0.30	3.00	2.50
U-2	200	8.0	100	8.0	–	–	–	0.50	–	–
C-2-1.25-1	200	8.0	100	8.0	250	185	8	0.50	1.00	1.25
D-2-1.25-1	200	8.0	100	8.0	250	185	8	0.50	1.00	1.25
C-2-1.25-2	200	8.0	100	8.0	250	185	16	0.50	2.00	1.25
D-2-1.25-2	200	8.0	100	8.0	250	185	16	0.50	2.00	1.25
C-2-1.25-3	200	8.0	100	8.0	250	185	24	0.50	3.00	1.25
D-2-1.25-3	200	8.0	100	8.0	250	185	24	0.50	3.00	1.25
C-2-2-1	200	8.0	100	8.0	400	185	8	0.50	1.00	2.00
D-2-2-1	200	8.0	100	8.0	400	185	8	0.50	1.00	2.00
C-2-2-2	200	8.0	100	8.0	400	185	16	0.50	2.00	2.00
D-2-2-2	200	8.0	100	8.0	400	185	16	0.50	2.00	2.00
C-2-2-3	200	8.0	100	8.0	400	185	24	0.50	3.00	2.00
D-2-2-3	200	8.0	100	8.0	400	185	24	0.50	3.00	2.00
C-2-2.5-1	200	8.0	100	8.0	500	185	8	0.50	1.00	2.50
D-2-2.5-1	200	8.0	100	8.0	500	185	8	0.50	1.00	2.50
C-2-2.5-2	200	8.0	100	8.0	500	185	16	0.50	2.00	2.50
D-2-2.5-2	200	8.0	100	8.0	500	185	16	0.50	2.00	2.50
C-2-2.5-3	200	8.0	100	8.0	500	185	24	0.50	3.00	2.50
D-2-2.5-3	200	8.0	100	8.0	500	185	24	0.50	3.00	2.50
U-3	200	8.0	150	8.0	–	–	–	0.75	–	–
C-3-1.25-1	200	8.0	150	8.0	250	185	8	0.75	1.00	1.25
D-3-1.25-1	200	8.0	150	8.0	250	185	8	0.75	1.00	1.25
C-3-1.25-2	200	8.0	150	8.0	250	185	16	0.75	2.00	1.25
D-3-1.25-2	200	8.0	150	8.0	250	185	16	0.75	2.00	1.25
C-3-1.25-3	200	8.0	150	8.0	250	185	24	0.75	3.00	1.25
D-3-1.25-3	200	8.0	150	8.0	250	185	24	0.75	3.00	1.25
C-3-2-1	200	8.0	150	8.0	400	185	8	0.75	1.00	2.00
D-3-2-1	200	8.0	150	8.0	400	185	8	0.75	1.00	2.00
C-3-2-2	200	8.0	150	8.0	400	185	16	0.75	2.00	2.00
D-3-2-2	200	8.0	150	8.0	400	185	16	0.75	2.00	2.00
C-3-2-3	200	8.0	150	8.0	400	185	24	0.75	3.00	2.00
D-3-2-3	200	8.0	150	8.0	400	185	24	0.75	3.00	2.00
C-3-2.5-1	200	8.0	150	8.0	500	185	8	0.75	1.00	2.50
D-3-2.5-1	200	8.0	150	8.0	500	185	8	0.75	1.00	2.50
C-3-2.5-2	200	8.0	150	8.0	500	185	16	0.75	2.00	2.50
D-3-2.5-2	200	8.0	150	8.0	500	185	16	0.75	2.00	2.50
C-3-2.5-3	200	8.0	150	8.0	500	185	24	0.75	3.00	2.50
D-3-2.5-3	200	8.0	150	8.0	500	185	24	0.75	3.00	2.50
U-4	200	8.0	100	12.5	–	–	–	0.50	1.00	–
C-4-1.25-1	200	8.0	100	12.5	250	185	8	0.50	1.00	1.25
D-4-1.25-1	200	8.0	100	12.5	250	185	8	0.50	1.00	1.25
C-4-1.25-2	200	8.0	100	12.5	250	185	16	0.50	2.00	1.25
D-4-1.25-2	200	8.0	100	12.5	250	185	16	0.50	2.00	1.25
C-4-1.25-3	200	8.0	100	12.5	250	185	24	0.50	3.00	1.25
D-4-1.25-3	200	8.0	100	12.5	250	185	24	0.50	3.00	1.25
C-4-2-1	200	8.0	100	12.5	400	185	8	0.50	1.00	2.00
D-4-2-1	200	8.0	100	12.5	400	185	8	0.50	1.00	2.00
C-4-2-2	200	8.0	100	12.5	400	185	16	0.50	2.00	2.00
D-4-2-2	200	8.0	100	12.5	400	185	16	0.50	2.00	2.00
C-4-2-3	200	8.0	100	12.5	400	185	24	0.50	3.00	2.00

Table 5 (continued)

Specimen	Chord member		Brace member		Reinforced plate			β	Δ	λ
	b_0 and h_0	t_0	b_1 and h_1	t_1	L_r	b_r	t_r			
D-4-2-3	200	8.0	100	12.5	400	185	24	0.50	1.00	2.00
C-4-2.5-1	200	8.0	100	12.5	500	185	8	0.50	1.00	2.50
D-4-2.5-1	200	8.0	100	12.5	500	185	8	0.50	2.00	2.50
C-4-2.5-2	200	8.0	100	12.5	500	185	16	0.50	2.00	2.50
D-4-2.5-2	200	8.0	100	12.5	500	185	16	0.50	3.00	2.50
C-4-2.5-3	200	8.0	100	12.5	500	185	24	0.50	3.00	2.50
D-4-2.5-3	200	8.0	100	12.5	500	185	24	0.50	0.33	2.50
U-5	200	8.0	120	8.0	–	–	–	0.60	–	–
C-5-2-2	200	8.0	120	8.0	400	185	16	0.60	2.00	2.00
D-5-2-2	200	8.0	120	8.0	400	185	16	0.60	2.00	2.00
U-6	200	8.0	160	8.0	–	–	–	0.80	–	–
C-6-2-2	200	8.0	160	8.0	400	185	16	0.80	2.00	2.00
D-6-2-2	200	8.0	160	8.0	400	185	16	0.80	2.00	2.00

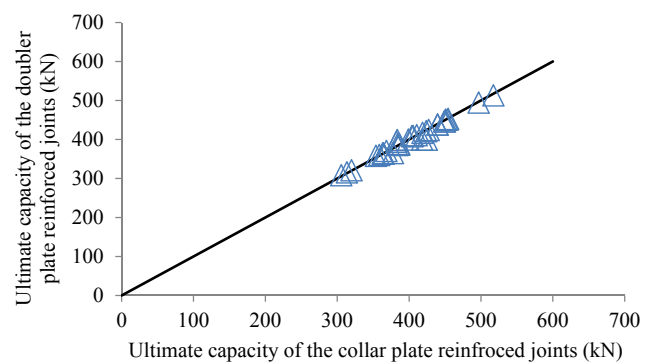


Fig. 11. Comparison for ultimate capacity between collar plate SHS T-joints and doubler plate SHS T-joints.

reinforced SHS T-joints in structural applications since it is easier to reinforce joints using a doubler plate rather than using a collar plate. Use of a doubler plate does not need to have a pocket in reinforcing plate. However, it is easier to reinforce SHS T-joints of structures in service by using collar plate.

3.2. Assessment of the geometrical parameters of the reinforcing plates

A parametric study was carried out to determine the effect of various geometrical parameters of the reinforcing plate and plate type on the ultimate capacity of SHS T-joints. As discussed in the previous section, test data showed that the type of reinforced plate (collar plate vs. doubler plate) has no influence on the ultimate capacity of the SHS T-joint. Therefore, only SHS T-joints reinforced with doubler plate were considered in the parametric study as discussed in this section.

Firstly, the effect of the reinforcing plate thickness was evaluated. Three different thicknesses were used: 8 mm, 16 mm and 24 mm. The chord member thickness for each case was kept unchanged at 8 mm (see in Table 5). Fig. 12 shows the relationship between the ratio of the reinforced plate thickness to chord member thickness (Δ) and the ratio of the ultimate capacity of reinforced joints to those of unreinforced joints (N_r/N_u). From this figure, it can be found that the capacity of the reinforced joint generally increases as the thickness of the reinforcing plate increases. This is due to the fact that the stiffness around the intersection area increases as the thickness of the reinforcing plate increases. However, the ultimate capacity of the reinforced joints converges when the thickness of the reinforcing plate is higher than twice the chord wall thickness. This is because the location of the failure moved away from the brace-chord intersection to the toe of the

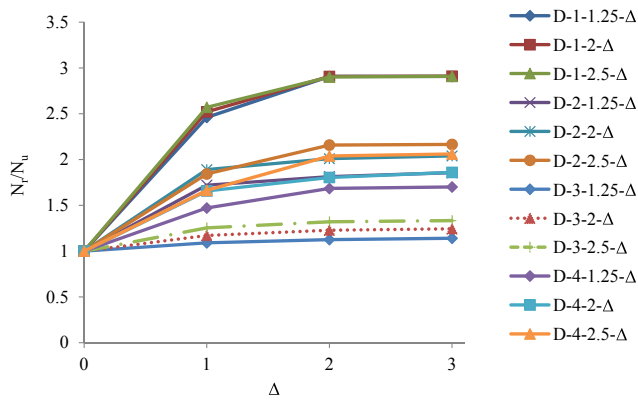


Fig. 12. Comparison of the effect of Δ on N_r/N_u .

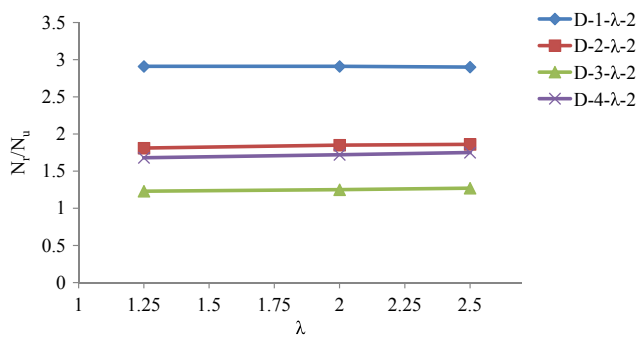


Fig. 13. Comparison of the effect of λ on N_r/N_u .

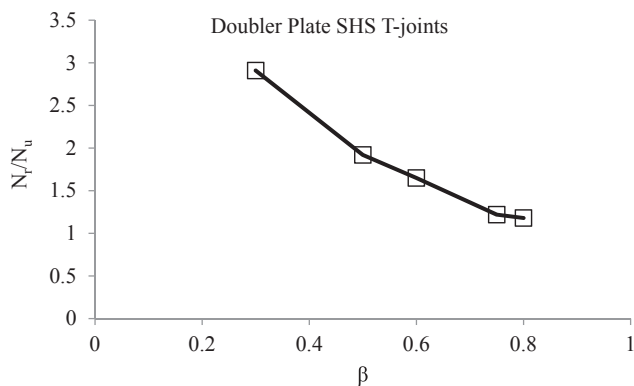


Fig. 14. Effect of β on the capacity ratio.

reinforcing plate. Hence, this study concludes that the ratio of the reinforced plate thickness to chord member thickness (Δ) larger than 2 provides no beneficial effect in terms of the strength of the SHS T-joint.

The second geometrical parameter was the ratio of reinforcing plate length to chord member width (λ). Three different λ values were used in the parametric study (1.25, 2 and 2.5) and a value of Δ was kept unchanged at 2.0. Since the Eurocode 3 EN 1993-1-8 [9] has limitations on the length of reinforced plate, the smaller value of λ is chosen as 1.25. As shown in Fig. 13, the value of λ has a negligible or no effect on the ultimate capacity of a reinforced joint. Hence, this study concludes that plate length as is Eq. (3) can be used and no changes are recommended.

3.3. Assessment of geometrical parameters of the tubular members

This section presents the effect of brace width to chord width ratio (β) on the ultimate capacity of reinforced SHS T-joints. As discussed in previous sections, the capacity of a reinforced joint was found to be independent of the reinforcing plate type (collar plate vs. doubler plate)

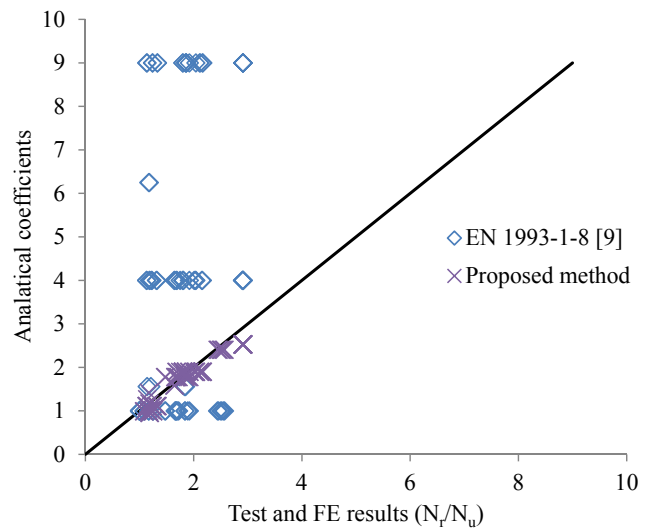


Fig. 15. Comparison of all results with the current design guideline and proposed method.

and the reinforcing plate length. The ultimate capacity of the SHS T-joint did not increase when the plate thickness exceeded twice that of the member. Therefore, D-1-2-2, D-2-2-2, D-3-2-2, D-5-2-2, and D-6-2-2 joints were compared in order to study the effect of the parameter, β on the ultimate capacity of the SHS T-joint.

Fig. 14 shows the effect of the brace-to-chord width ratio (β) to the ratio of the ultimate capacity of the reinforced joint to that of the unreinforced joint (N_r/N_u). It can be found that as the value of β increases, the ultimate capacity decreases. This decreasing trend becomes insignificant when the value of the β exceeds 0.75. This indicates that the rate of increase in stiffness of the intersectional area is higher when the β value decreases and approaches 0.30, on the other hand, an increasing in β value beyond 0.75 provides no additional stiffness in the intersectional area and thus, it provides no additional benefits. Therefore, this study found that the beneficial effect of reinforcing the chord member using a reinforcing plate is present when the brace-to-chord (β) width ratio is in between 0.30 and 0.75.

3.4. Proposed design method

The parametric study revealed that the effect of the reinforcing plate type and length on the ultimate load carrying capacity of SHS T-joints were insignificant as the range of validity in CIDECT guide No. 3 [17] and EN 1993-1-8 [9] applied for reinforcing plate and main members. However, the capacity of a reinforced joint significantly improved as the thickness of the reinforcing plate increased until it reached a value of twice the thickness of the chord member. Another parameter which directly affected the joint capacity was brace-to-chord width ratio (β).

Aforementioned, the current method in the Eurocode EN 1993-1-8 [9] predicts the capacity of a reinforced joint using the design equation developed for the unreinforced tubular joint. No rational or research data is available to support this design philosophy. The current study found that such design method for predicting the capacity of a reinforced SHS T-joint is unconservative and may lead to premature failure of an SHS T-joint.

Based on the outcomes of the current study, a correction factor (ψ) is recommended for the design equation of the Eurocode EN 1993-1-8 [9] available for unreinforced SHS T-joint. This correction factor was determined from multiple linear regression analyses undertaken using the statistical software package, SPSS [31]. Values of the dependent variable (ψ) and the independent variables (Δ and β) were imported in the form of a matrix. The following equation was derived for calculating the capacity of the reinforced SHS T-joint under axial brace compressive load.

$$N_r = \psi N_u \quad (6)$$

where ψ is the correction factor for the collar plate and doubler plate reinforced SHS T-joints. The correction factor (ψ) was determined using the outcomes of FE analyses and experimental tests as shown in the following equation.

$$\psi = 3.227 - 3.143\beta + 0.121\Delta \quad (7)$$

The accuracy of the proposed method was checked against both the test and FE results obtained in the current study. Fig. 15 illustrates the comparison between the data obtained from this study and the analytical coefficients (ψ for the proposed method and N_r/N_u for EN 1993-1-8). It can be found that the results of the Eurocode EN 1993-1-8 [9] either overestimates or underestimates the capacity of SHS T-joints reinforced with doubler plate and collar plate. A good agreement exists between the design method (proposed Eqs. (6) and (7)) and the results obtained, with an average ratio of the predicted to the observed capacity of 0.95 and a standard deviation of 0.10.

4. Conclusions

This paper presented the results of both the experimental work and an extensive parametric study on the strength of welded steel SHS joints reinforced with two different types of reinforcing plate (collar plate vs. doubler plate) and various geometric parameters for the members and as well as for the reinforcing plate. A new design equation for predicting the capacity of reinforced SHS T-joints has been developed, validated, and proposed. The geometrical parameters for both the reinforcing plate and main members have been chosen in accordance with CIDECT guide No. 3 [17] and EN 1993-1-8 [9]. The following conclusions are drawn based on the outcomes of this study, however, these conclusions may be limited to the scope of work of the study.

- (1) The typical failure mode of SHS T-joints reinforced with collar and doubler plates was found to be due to plastification of the chord face when the brace member of the joint was subjected axial compressive load.
- (2) The behaviour of SHS T-joints reinforced with two different plate types namely, collar plate and doubler plate were very similar.
- (3) The ultimate capacity of the reinforced SHS T-joint significantly increased compared to the corresponding unreinforced joint. However, this beneficial effect diminished when reinforcing plate thickness increased beyond twice the chord member thickness.
- (4) It is unconservative and thus, unsafe to use design equations of EN 1993-1-8 for determining the capacity of the reinforced joints. These equations were developed for determining the strength of unreinforced joints and thus, by simply replacing the chord member thickness with the reinforcing plate thickness may lead to an erroneous prediction in the capacity of the reinforced joints.
- (5) The current study developed and proposed a new design equation that can be safely used for estimating the capacity of the SHS T-joints reinforced with collar plate and doubler plate when subjected to brace axial compressive load. However, it should be noted that the design equation presented in this paper does not take into account any safety factor and the geometrical parameters beyond the validity range defined in the current design guidelines.

Acknowledgments

The experimental tests were carried out in the Structural Engineering Laboratory of Windsor University, Canada and with the financial assistance of NSERC located in Ottawa, Canada. The authors

express their special thanks for Eric Hughes, Jothiarun Dhanapal, and Soham Mitra who helped preparing the test specimens and undertaking the tests in the lab.

References

- [1] Qu H, Huo J, Xu C, Fu F. Numerical studies on dynamic behavior of tubular T-joint subjected to impact loading. *Int J Imp Eng* 2014;67:12–26.
- [2] Shao Y-B, Lie S-T, Chiew S-P. Static strength of tubular T-joints with reinforced chord under axial compression. *Adv Struct Eng* 2010;13:369–77.
- [3] Nassiraei H, Lotfollahi-Yaghin MA, Ahmadi H, Zhu L. Static strength of doubler plate reinforced tubular T/Y-joints under in-plane bending load. *J Constr Steel Res* 2017;136:49–64.
- [4] Gao F, Guan X-Q, Zhu H-P, Liu X-N. Fire resistance behaviour of tubular T-joints reinforced with collar plates. *J Constr Steel Res* 2015;115:106–20.
- [5] Lesani M, Bahaari M, Shokrieh M. Experimental investigation of FRP-strengthened tubular T-joints under axial compressive loads. *Constr Build Mater* 2014;53:243–52.
- [6] Qu H, Li A, Huo J, Liu Y. Dynamic performance of collar plate reinforced tubular T-joint with precompression chord. *Eng Struct* 2017;141:555–70.
- [7] Lesani M, Bahaari M, Shokrieh M. Numerical investigation of FRP-strengthened tubular T-joints under axial compressive loads. *Compos Struct* 2013;100:71–8.
- [8] Feng R, Chen Y, Chen D. Experimental and numerical investigations on collar plate and doubler plate reinforced SHS T-joints under axial compression. *Thin-Wall Struct* 2017;110:75–87.
- [9] CEN. Design of Steel Structures. In: Part; editor. EN 1993-1-8-Design of Joints. London: British Standard Institute; 2005.
- [10] Yang J, Shao Y, Chen C. Static strength of chord reinforced tubular Y-joints under axial loading. *Mar struct* 2012;29:226–45.
- [11] Van der Vegte G, Choo Y, Liang J, Zettlemoyer N, Liew J. Static strength of T-joints reinforced with doubler or collar plates. II: numerical simulations. *J Struct Eng* 2005;131:129–38.
- [12] Choo Y, Liang J, Van der Vegte G, Liew J. Static strength of doubler plate reinforced CHS X-joints loaded by in-plane bending. *J Constr Steel Res* 2004;60:1725–44.
- [13] Fung T, Chan T, Soh C. Ultimate capacity of doubler plate-reinforced tubular joints. *J Struct Eng* 1999;125:891–9.
- [14] Gao F, Guan X-Q, Zhu H-P, Xia Y. Hysteretic behaviour of tubular T-joints reinforced with doubler plates after fire exposure. *Thin-Wall Struct* 2015;92:10–20.
- [15] Nazari A, Guan Z, Daniel W, Gurgenci H. Parametric study of hot spot stresses around tubular joints with doubler plates. *Prac Period Struct Des Construct* 2007;12:38–47.
- [16] Li W, Zhang S, Huo W, Bai Y, Zhu L. Axial compression capacity of steel CHS X-joints strengthened with external stiffeners. *J Constr Steel Res* 2018;141:156–66.
- [17] Packer JA, Wardenier J, Zhao X-L, van der Vegte GJ, Kurobane Y. Design guide for rectangular hollow section (RHS) joints under predominantly static loading. Second ed: Verlag TÜV Rheinland. 2009.
- [18] Shao Y-B, Li T, Lie S-T, Chiew S-P. Hysteretic behaviour of square tubular T-joints with chord reinforcement under axial cyclic loading. *J Constr Steel Res* 2011;67:140–9.
- [19] Lu LHGD, De Winkel Y, Yu J. Wardenier Deformation limit for the ultimate strength of hollow section joints. *Proceedings of the Sixth International Symposium on Tubular Structures. Melbourne, Australia. 1994.*
- [20] Kurobane Y, Makino Y, Ochi K. Ultimate resistance of unstiffened tubular joints. *J Struct Eng* 1984;110:385–400.
- [21] ABAQUS/Standard. In: Ed, editor. K a S Hibbit;. Version 6.14-1 ed. USA: K. a. S. Hibbit; 2014.
- [22] Wang C, Chen Y, Chen X, Chen D. Experimental and numerical research on out-of-plane flexural property of plates reinforced SHS X-joints. *Thin-Wall Struct* 2015;94:466–77.
- [23] Chen Y, Chen D. Ultimate capacities formulae of collar and doubler plates reinforced SHS X-joints under in-plane bending. *Thin-Wall Struct* 2016;99:21–34.
- [24] Boresi AP, Schmidt R, J. *Advanced mechanics of materials*. 6th Ed. ed: John Wiley and Sons; 2003.
- [25] Wardenier J, Kurobane Y, Packer JA, van der Vegte GJ, Zhao X-L. Design guide for circular hollow section (CHS) joints under predominantly static loading. Second ed: Cidect; 2008.
- [26] Van der Vegte G, Wardenier J, Zhao X, Packer J. Evaluation of new CHS strength formulae to design strengths. *Proceedings of the 12th international symposium on tubular structures, Shanghai, China Taylor & Francis, Group. 2008. p. 313–22.*
- [27] Van der Vegte G, Makino Y. Ultimate strength formulation for axially loaded CHS uniplanar T-joints. *The Fifteenth International Offshore and Polar Engineering Conference: International Society of Offshore and Polar Engineers. 2005.*
- [28] Wardenier J, van der Vegte G, Liu D. Chord stress function for rectangular hollow section X and T joints. *The Seventeenth International Offshore and Polar Engineering Conference International Society of Offshore and Polar Engineers. 2007.*
- [29] Ozyurt E, Wang Y, Tan K. Elevated temperature resistance of welded tubular joints under axial load in the brace member. *Eng Struct* 2014;59:574–86.
- [30] Nassiraei H, Lotfollahi-Yaghin MA, Ahmadi H. Static strength of collar plate reinforced tubular T/Y-joints under brace compressive loading. *J Constr Steel Res* 2016;119:39–49.
- [31] SPSS. Version 11.0 Chicago (IL): SPSS Inc. 2004.